Fragmentation Functions at Belle and Belle II

Simon Schneider

12th Circum-Pan-Pacific Symposium on High Energy Spin Physics
November 12th 2024 - Hefei, Anhui

Research supported by:

Fragmentation Functions at Belle and Belle II

- How the Belle and Belle II experiments are designed
- Fragmentation function results from Belle data
- Currently ongoing studies
- Near-future opportunities

Long history of studying QCD in e^+e^- experiments

E.g. PETRA at DESY: Discovery of the gluon (1979)

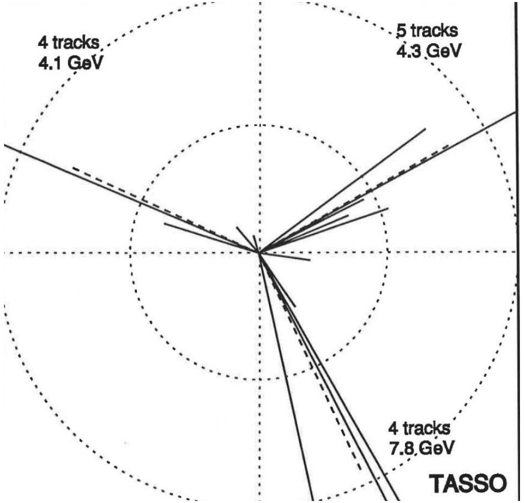

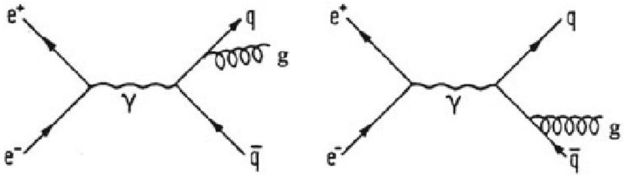

Fig. 1. Feynman diagrams for hard gluon bremsstrahlung $e^+e^- \to q\bar{q}g$.

Image source: Söding, P. (2010). On the discovery of the gluon. *The European Physical Journal H*, *35*(1), 3-28.

The less distant past: Belle at the KEKB e^+e^- collider (1999-2010)

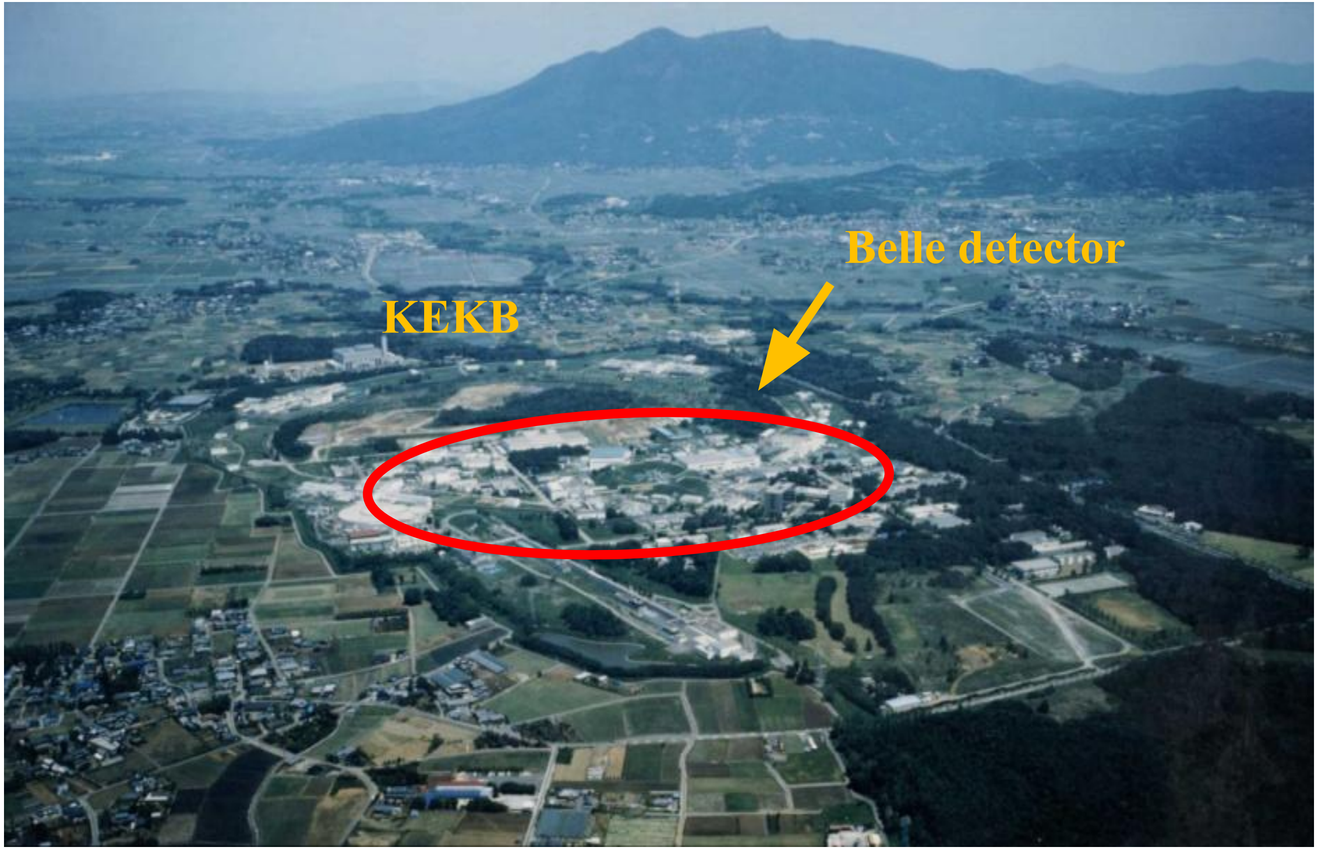

AERIAL VIEW OF EXPERIMENT

Belle Detector

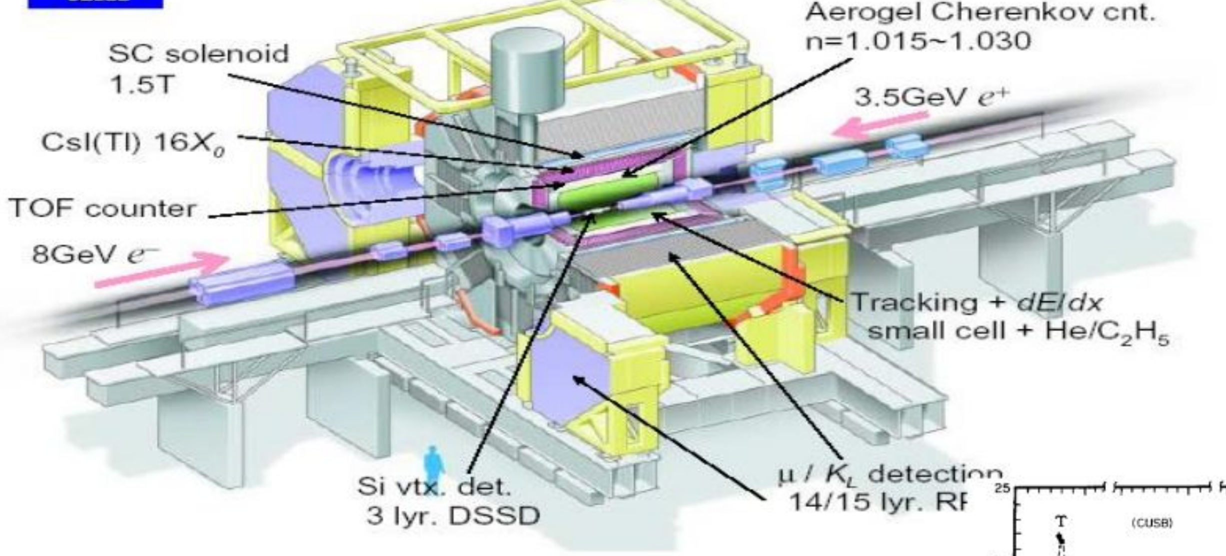

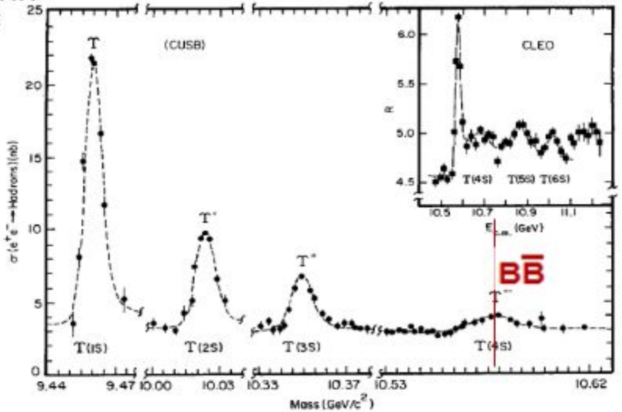

Exp.	Scans / Off-res. fb^{-1}	$\Upsilon(5S)$ 10876 MeV fb^{-1}	10^6	$\Upsilon(4S)$ 10580 MeV fb^{-1}	10^6	$\Upsilon(3S)$ 10355 MeV fb^{-1}	10^6	$\Upsilon(2S)$ 10023 MeV fb^{-1}	10^6	$\Upsilon(1S)$ 9460 MeV fb^{-1}	10^6
CLEO	17.1	0.4	0.1	16	17.1	1.2	5	1.2	10	1.2	21
BaBar	54	R_b scan		433	471	30	122	14	99	–	
Belle	100	121	36	711	772	3	12	25	158	6	102

From: *PTEP* 2019 (2019) 12, 123C01, *PTEP* 2020 (2020) 2, 029201

+About 4x10^6 events per fb^{-1} off-resonance

SuperKEKB

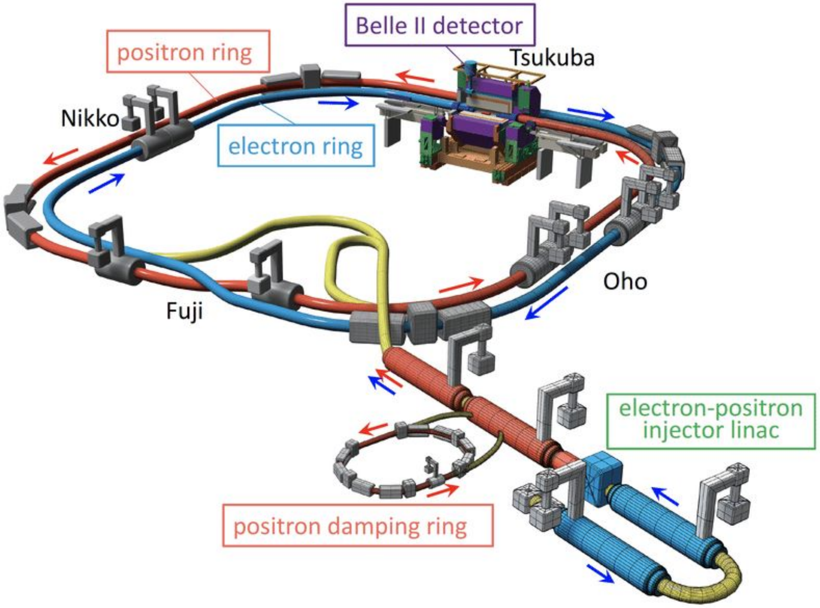

Upgrade from KEKB to increase luminosity
Design beam currents increased
Main increase from much smaller beam sizes

Nanobeam collision scheme

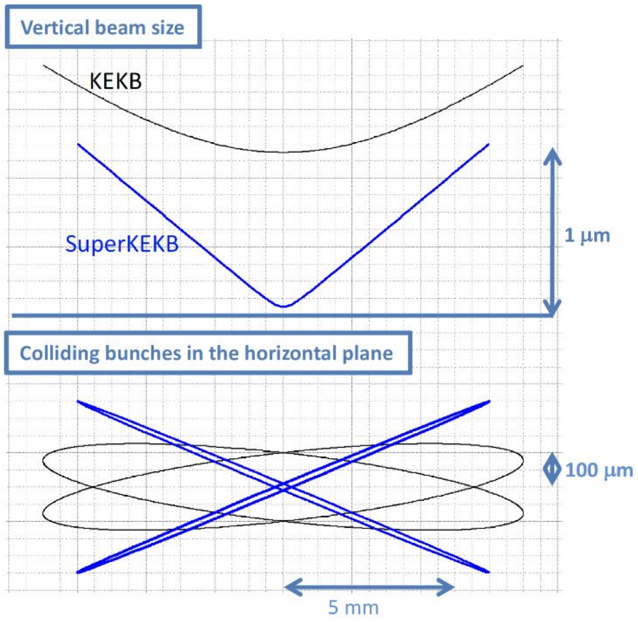

image source: Akai, K., Furukawa, K., & Koiso, H. (2018). SuperKEKB collider. Nuclear Instruments and Methods in Physics Research Section A: Accelerators, Spectrometers, Detectors and Associated Equipment, 907, 188-199.

Next Generation B-factory

BELLE II at SuperKEKB

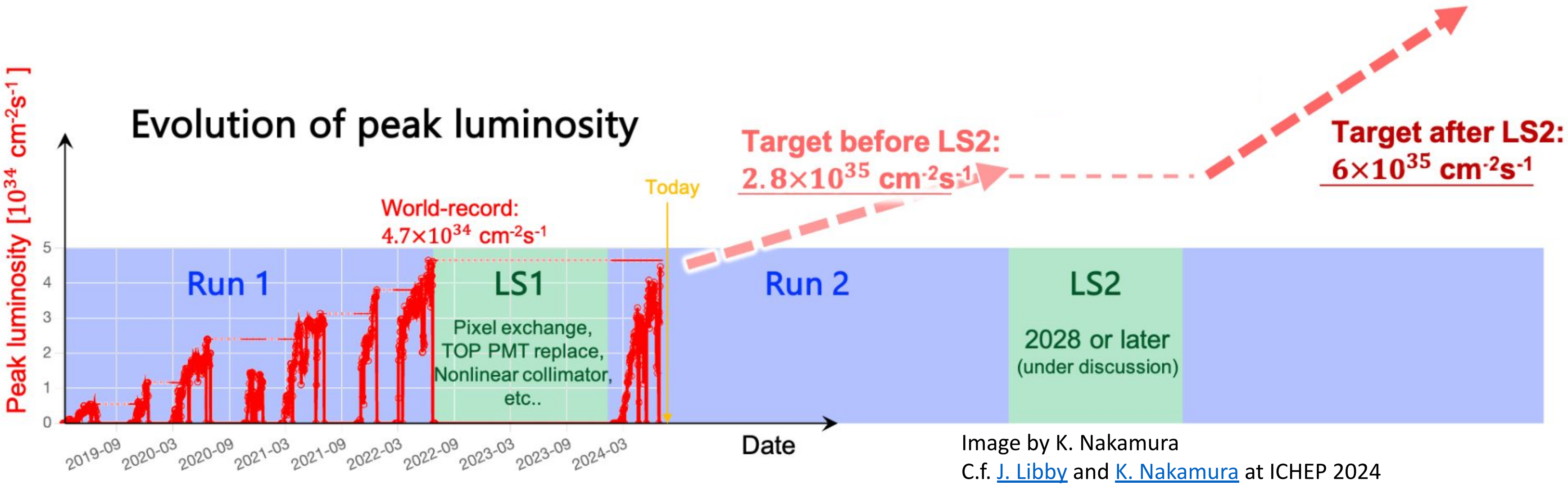

Image by K. Nakamura
C.f. J. Libby and K. Nakamura at ICHEP 2024

SuperKEKB delivered 4.7 x 10^{34} $cm^{-2}s^{-1}$ world record instantaneous luminosity

Belle II scheduled to drastically increase available data over the next few years

BELLE II EXPERIMENT

THE DETECTOR

- The upgraded Belle II began taking data in 2019:
  - **Vertex Detector (VXD)**: two innermost silicon strips replaced with pixel detectors
  - **Central Drift Chamber (CDC)**: smaller drift cells, reaches smaller radii
  - **Time Of Propagation (TOP)**: replaced TOF
  - **Aerogel Ring Imaging Cherenkov Detector (ARICH)**: replaced endcap ACC
  - **Electromagnetic Calorimeter (ECL)**: electronics upgrade
  - **K_L Muon Detector (KLM)**: two innermost barrel RPCs and endcaps replaced with scintillators

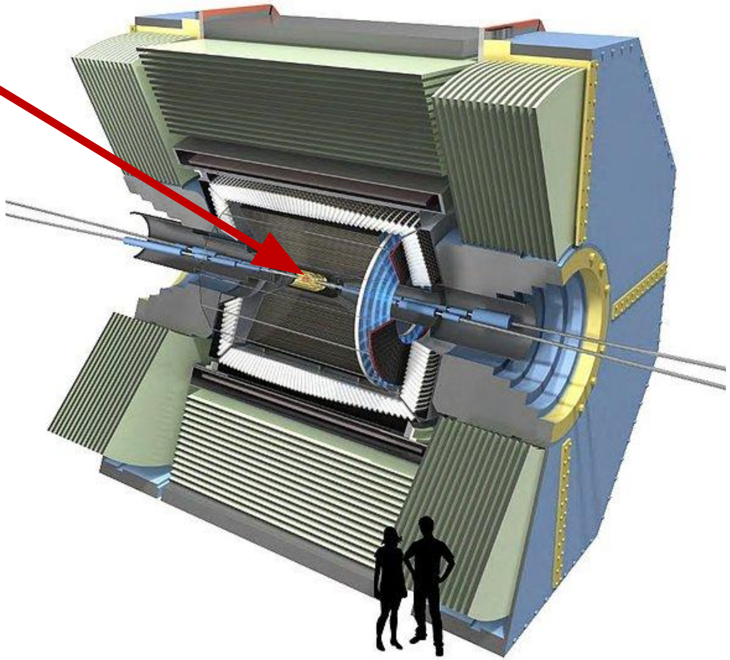

BELLE II EXPERIMENT

THE DETECTOR

- The upgraded Belle II began taking data in 2019:
  - **Vertex Detector (VXD)**: two innermost silicon strips replaced with pixel detectors
  - **Central Drift Chamber (CDC)**: smaller drift cells, reaches smaller radii
  - **Time Of Propagation (TOP)**: replaced TOF
  - **Aerogel Ring Imaging Cherenkov Detector (ARICH)**: replaced endcap ACC
  - **Electromagnetic Calorimeter (ECL)**: electronics upgrade
  - **K_L Muon Detector (KLM)**: two innermost barrel RPCs and endcaps replaced with scintillators

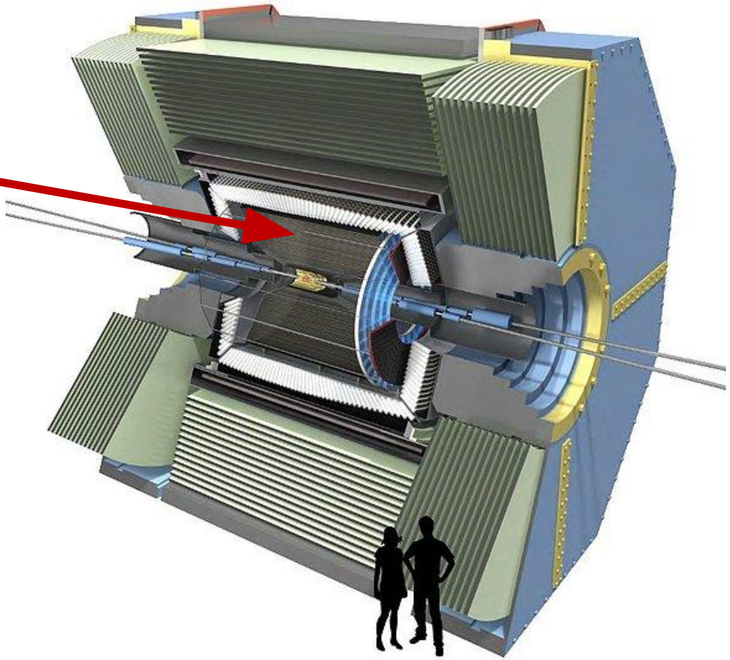

BELLE II EXPERIMENT

THE DETECTOR

- The upgraded Belle II began taking data in 2019:
  - **Vertex Detector (VXD)**: two innermost silicon strips replaced with pixel detectors
  - **Central Drift Chamber (CDC)**: smaller drift cells, reaches smaller radii
  - **Time Of Propagation (TOP)**: replaced TOF
  - **Aerogel Ring Imaging Cherenkov Detector (ARICH)**: replaced endcap ACC
  - **Electromagnetic Calorimeter (ECL)**: electronics upgrade
  - **K_L Muon Detector (KLM)**: two innermost barrel RPCs and endcaps replaced with scintillators

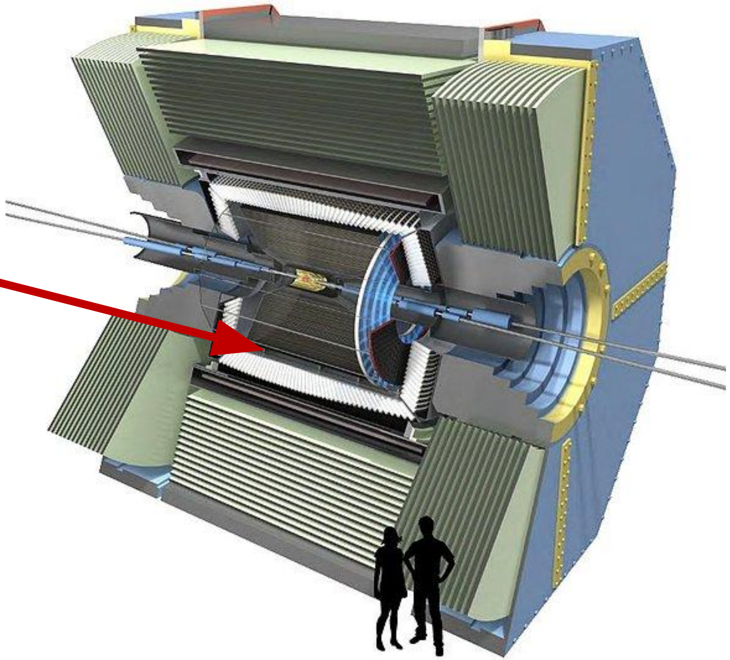

BELLE II EXPERIMENT

THE DETECTOR

- The upgraded Belle II began taking data in 2019:
  - **Vertex Detector (VXD)**: two innermost silicon strips replaced with pixel detectors
  - **Central Drift Chamber (CDC)**: smaller drift cells, reaches smaller radii
  - **Time Of Propagation (TOP)**: replaced TOF
  - **Aerogel Ring Imaging Cherenkov Detector (ARICH)**: replaced endcap ACC
  - **Electromagnetic Calorimeter (ECL)**: electronics upgrade
  - **K_L Muon Detector (KLM)**: two innermost barrel RPCs and endcaps replaced with scintillators

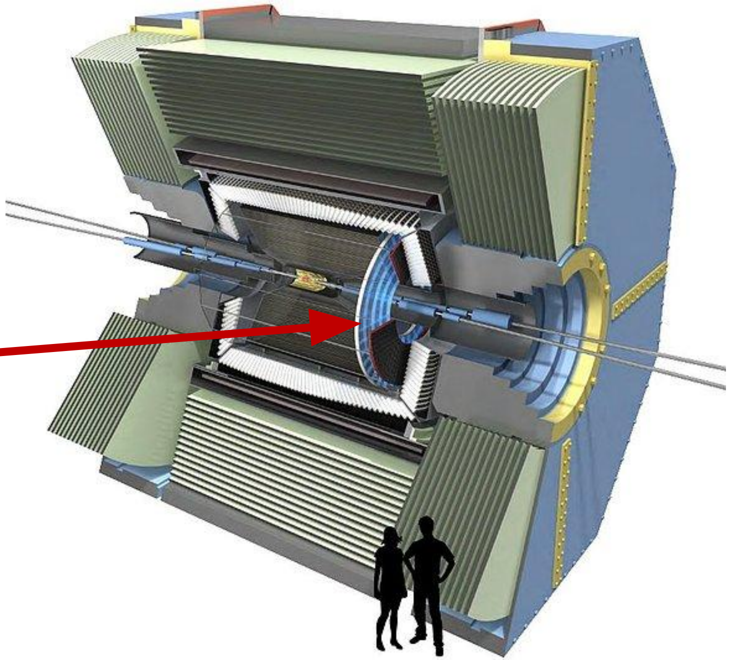

BELLE II EXPERIMENT

THE DETECTOR

- The upgraded Belle II began taking data in 2019:
  - **Vertex Detector (VXD)**: two innermost silicon strips replaced with pixel detectors
  - **Central Drift Chamber (CDC)**: smaller drift cells, reaches smaller radii
  - **Time Of Propagation (TOP)**: replaced TOF
  - **Aerogel Ring Imaging Cherenkov Detector (ARICH)**: replaced endcap ACC
  - **Electromagnetic Calorimeter (ECL)**: electronics upgrade
  - **K_L Muon Detector (KLM)**: two innermost barrel RPCs and endcaps replaced with scintillators

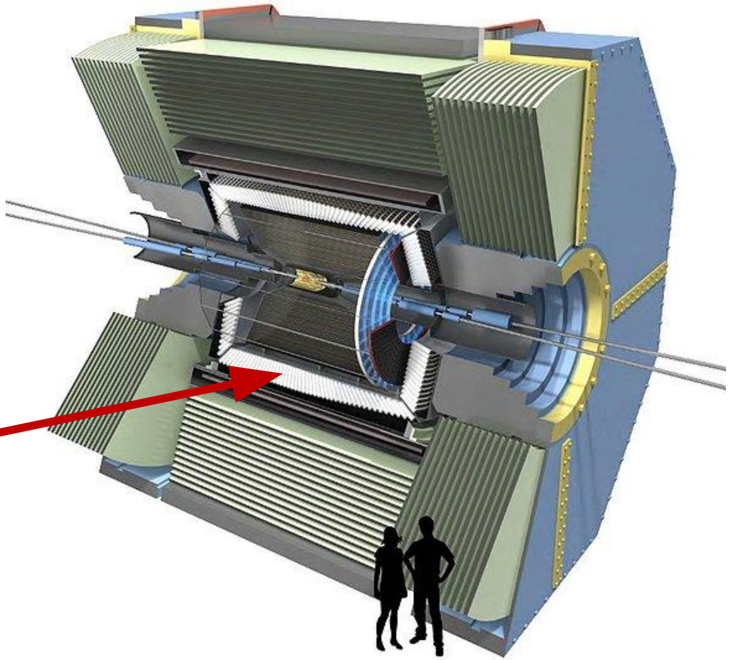

BELLE II EXPERIMENT

THE DETECTOR

- The upgraded Belle II began taking data in 2019:
  - **Vertex Detector (VXD)**: two innermost silicon strips replaced with pixel detectors
  - **Central Drift Chamber (CDC)**: smaller drift cells, reaches smaller radii
  - **Time Of Propagation (TOP)**: replaced TOF
  - **Aerogel Ring Imaging Cherenkov Detector (ARICH)**: replaced endcap ACC
  - **Electromagnetic Calorimeter (ECL)**: electronics upgrade
  - **K_L Muon Detector (KLM)**: two innermost barrel RPCs and endcaps replaced with scintillators

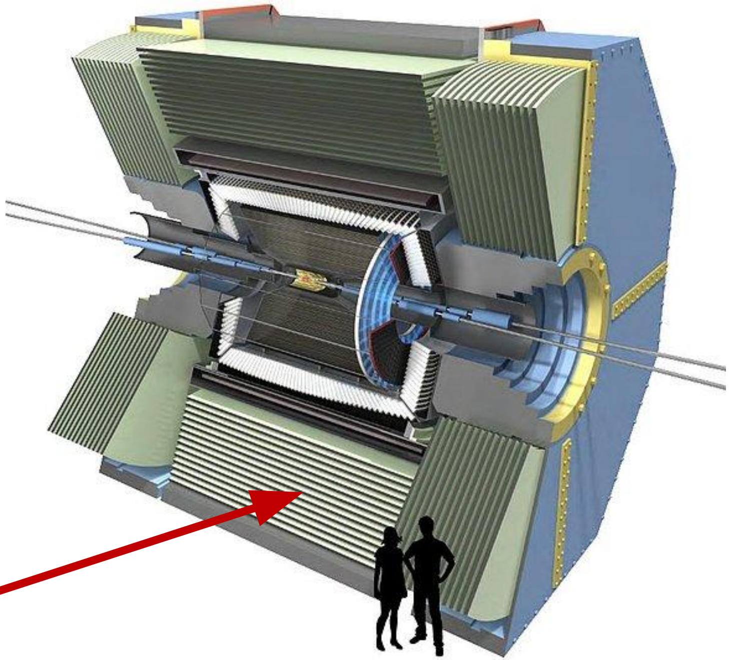

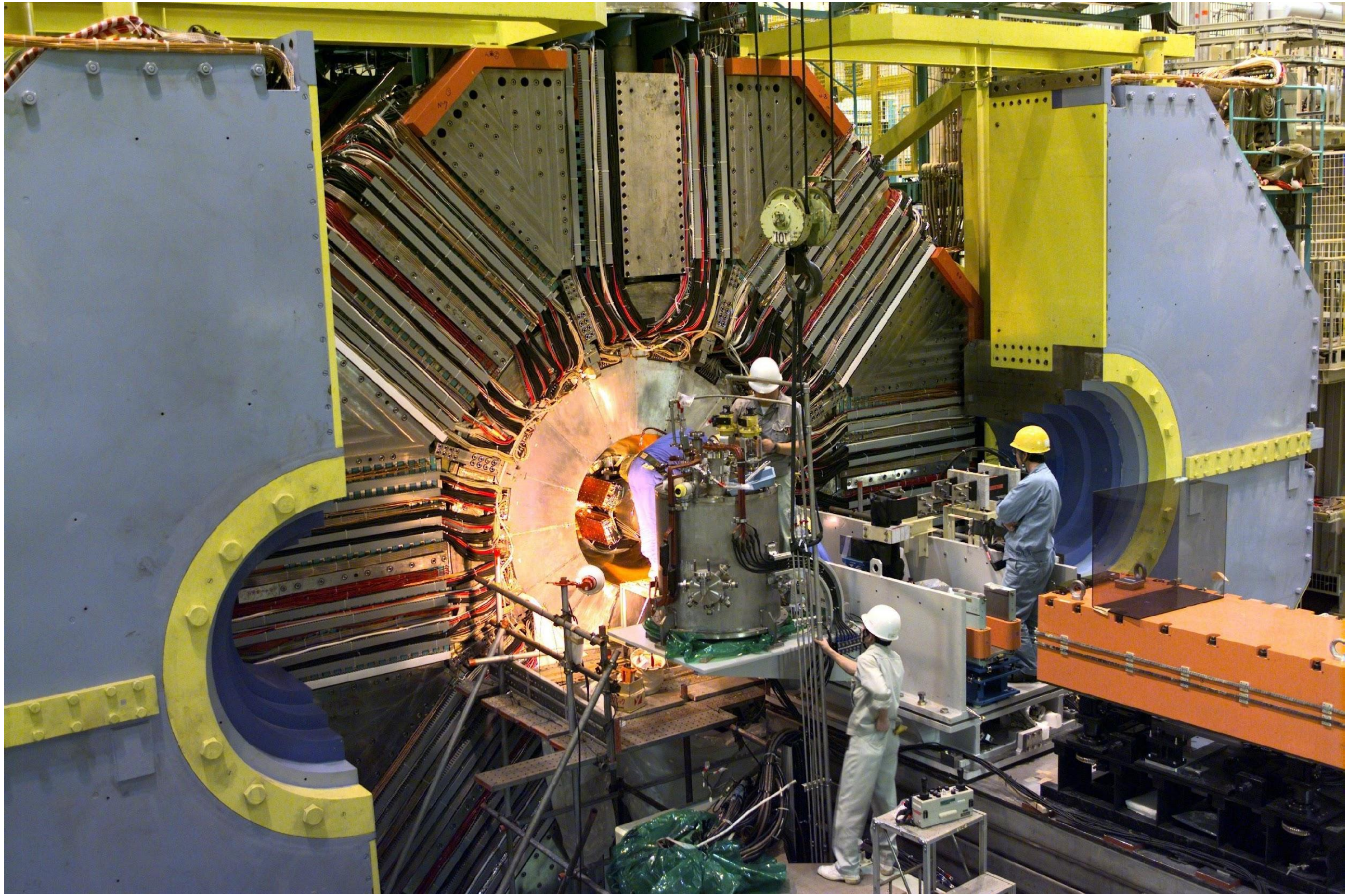

BELLE

FRAGMENTATION FUNCTIONS

INTRODUCTION

Encode the non-perturbative link between perturbative QCD processes and the observed final state particles

(light hadron) FFs can't be calculated from pQCD

→ Need to observe in experiment

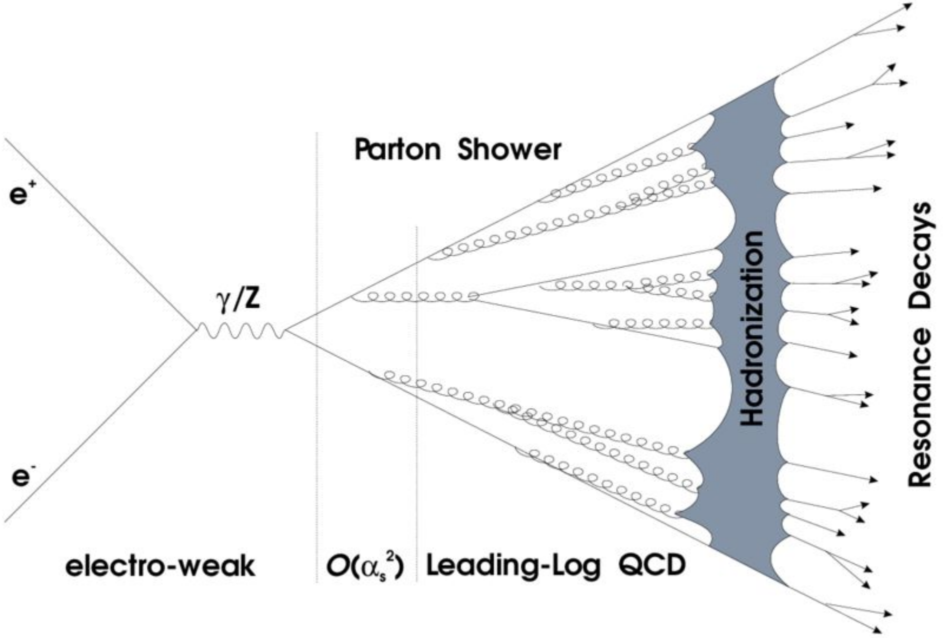

image source: Buskulic et al. (1995)

FRAGMENTATION FUNCTIONS

FACTORIZATION

Scattering amplitudes can be factorized into a perturbatively calculable part, $\hat{\sigma}$, and a non-perturbatively calculable part:

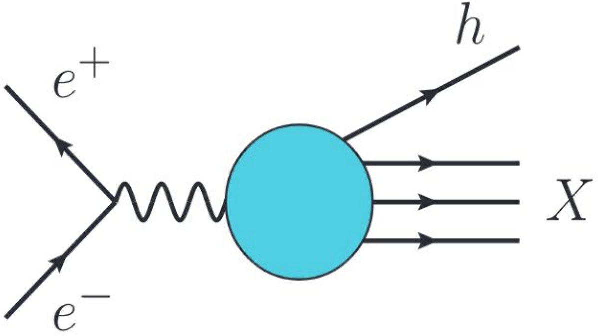

Single-inclusive annihilation:

$$\sigma^{e^+e^- \to hX} = \hat{\sigma} \otimes FF$$

Semi-inclusive deep inelastic scattering (SIDIS):

$$\sigma^{\ell N \to \ell hX} = \hat{\sigma} \otimes PDF \otimes FF$$

Single-inclusive proton-proton scattering:

$$\sigma^{pp \to hX} = \hat{\sigma} \otimes PDF \otimes PDF \otimes FF$$

FRAGMENTATION FUNCTIONS

FACTORIZATION

Scattering amplitudes can be factorized into a perturbatively calculable part, $\hat{\sigma}$, and a non-perturbatively calculable part:

Single-inclusive annihilation:

$\sigma^{e^+e^-\to hX} = \hat{\sigma} \otimes FF$

Semi-inclusive deep inelastic scattering (SIDIS):

$\sigma^{\ell N\to \ell hX} = \hat{\sigma} \otimes PDF \otimes FF$

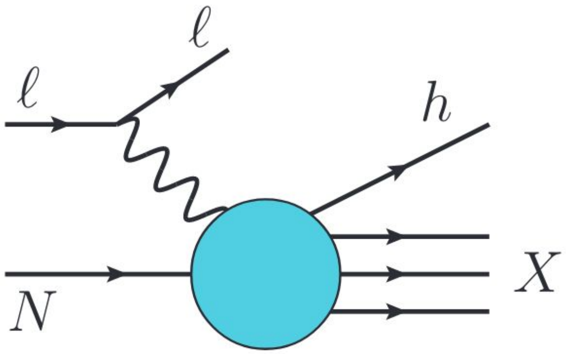

Single-inclusive proton-proton scattering:

$\sigma^{pp\to hX} = \hat{\sigma} \otimes PDF \otimes PDF \otimes FF$

FRAGMENTATION FUNCTIONS

FACTORIZATION

Scattering amplitudes can be factorized into a perturbatively calculable part, $\hat{\sigma}$, and a non-perturbatively calculable part:

Single-inclusive annihilation:

$$\sigma^{e^+e^-\to hX} = \hat{\sigma} \otimes FF$$

Semi-inclusive deep inelastic scattering (SIDIS):

$$\sigma^{\ell N\to \ell hX} = \hat{\sigma} \otimes PDF \otimes FF$$

Single-inclusive proton-proton scattering:

$$\sigma^{pp\to hX} = \hat{\sigma} \otimes PDF \otimes PDF \otimes FF$$

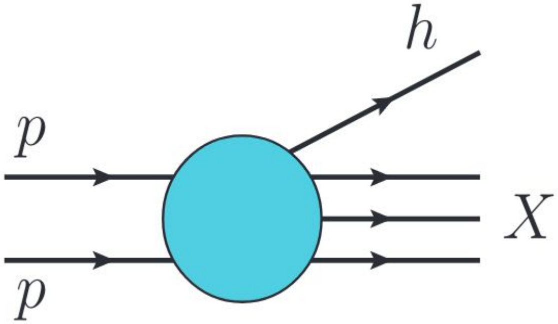

FRAGMENTATION FUNCTIONS

TRANSVERSE MOMENTUM DEPENDENCE

More than one degree of freedom

$$f(x) \rightarrow f(x, \vec{k}_T)$$

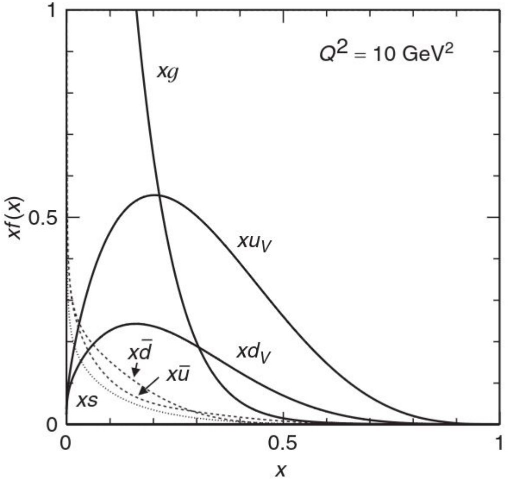

source: Mark Thomson "Modern Particle Physics"

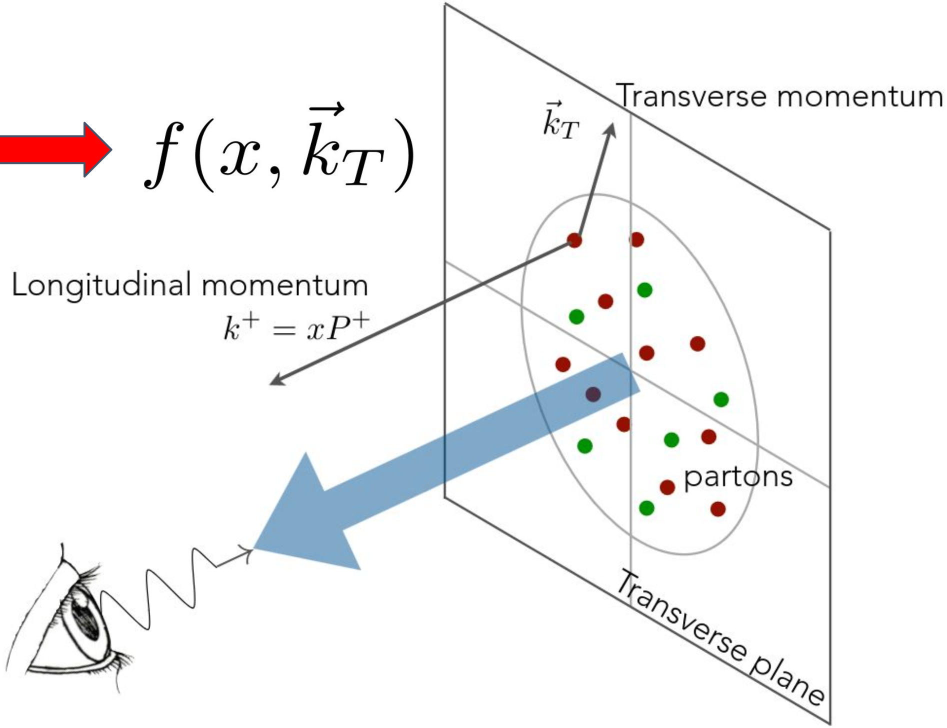

source: https://indico.cern.ch/event/797767/contributions/3682621/

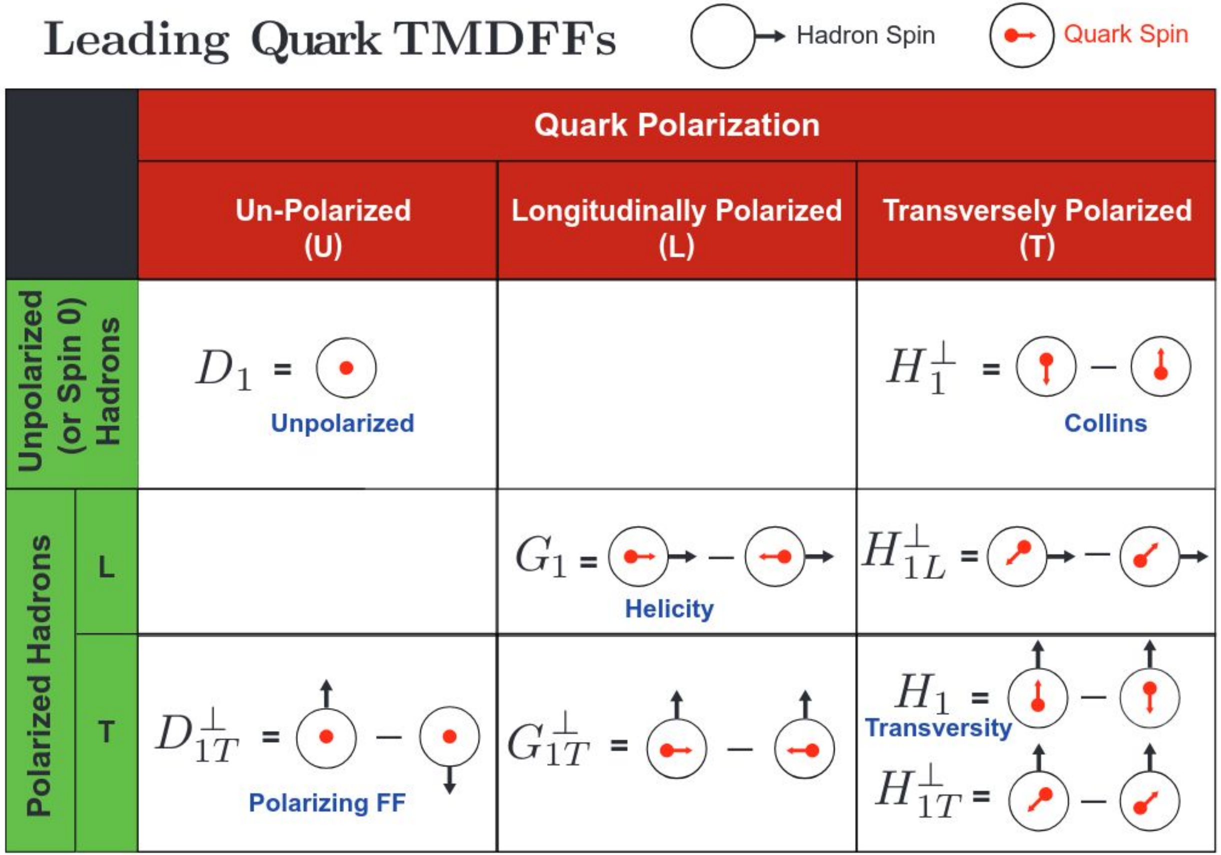

Image source: TMD handbook

Figure 2.6: Leading power quark TMD fragmentation functions for a spin-1/2 (or for an unpolarized or spin 0) hadron.

Determining final state polarization needs self-analyzing decays (Λ) -> Belle II Strength!

R. Seidl et al., "Update of inclusive cross sections of single and pairs of identified light charged hadrons", *Phys.Rev.D* 101 (2020) 9, 092004

- Used an updated ISR correction procedure
- Alternative fractional energy definitions were considered
  - Conventional: $z_i = 2E_{h,i} \,/\, \sqrt{s}$
  - AEMP: $z_1 = \frac{2P_1 \cdot q}{q^2}$, $z_2 = \frac{P_1 \cdot P_2}{P_1 \cdot q}$
  - MVH: $z_1 = \left(P_1 \cdot P_2 - \frac{M_{h1}^2 M_{h2}^2}{P_1 \cdot P_2}\right) \frac{1}{P_2 \cdot q - M_{h2}^2 \frac{P_1 \cdot q}{P_1 \cdot P_2}}$,

$$z_2 = \left(P_2 \cdot P_1 - \frac{M_{h2}^2 M_{h1}^2}{P_2 \cdot P_1}\right) \frac{1}{P_1 \cdot q - M_{h1}^2 \frac{P_2 \cdot q}{P_2 \cdot P_1}}$$

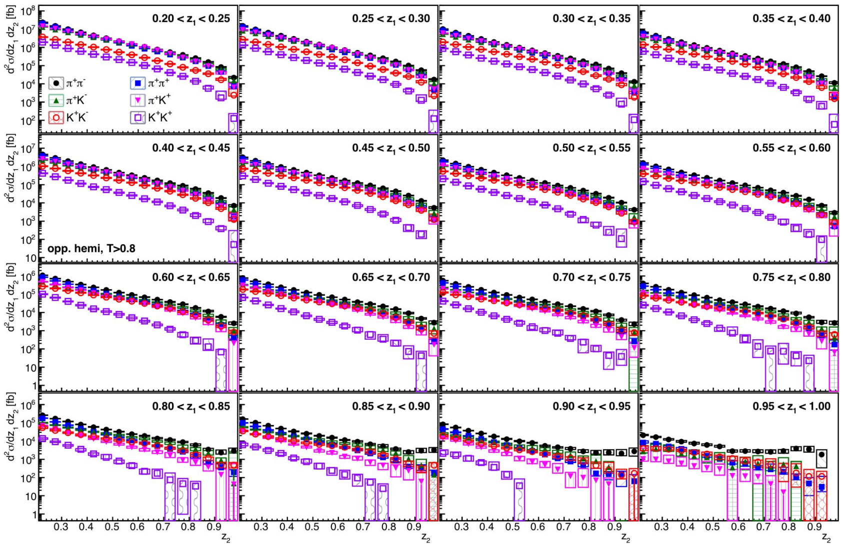

Differential cross sections of charged hadron pairs in opposite hemispheres, binned by conventional fractional energy

BELLE RESULTS
RECENT PUBLICATIONS

H. Li, A. Vossen, et al., “Azimuthal asymmetries of back-to-back $\pi^{\pm} - (\pi^{0}, \eta, \pi^{\pm})$ pairs in $e^{+}e^{-}$ annihilation”, *Phys.Rev.D* 100 (2019) 9, 092008

- The first observation of azimuthal asymmetries of pairs of back-to-back hadrons, one a charged pion and the other a π^0, $\pi^{\pm}$, or η meson
- Measurements are sensitive to the Collins fragmentation function, $H_1^{\perp}$

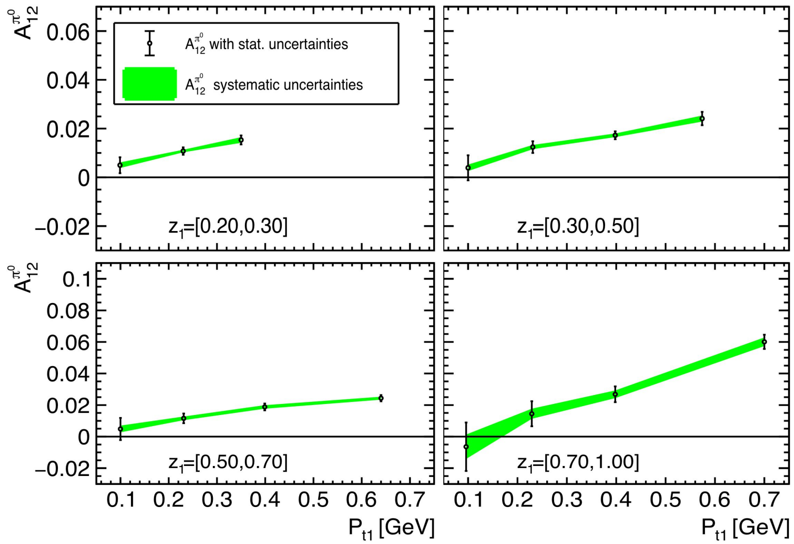

Azimuthal asymmetry of π^0 events binned by fractional energy, z

BELLE RESULTS

RECENT PUBLICATIONS

R. Seidl et al., "Transverse momentum dependent production cross sections of charged pions, kaons and protons produced in inclusive e^+e^- annihilation at $\sqrt{s}$ = 10.58 GeV", *Phys.Rev.D* 99 (2019) 11, 112006

- Production cross sections of charged pions, kaons, and protons as a function of fractional energy, thrust, and transverse momentum
- Measurements access the transverse momenta created during fragmentation

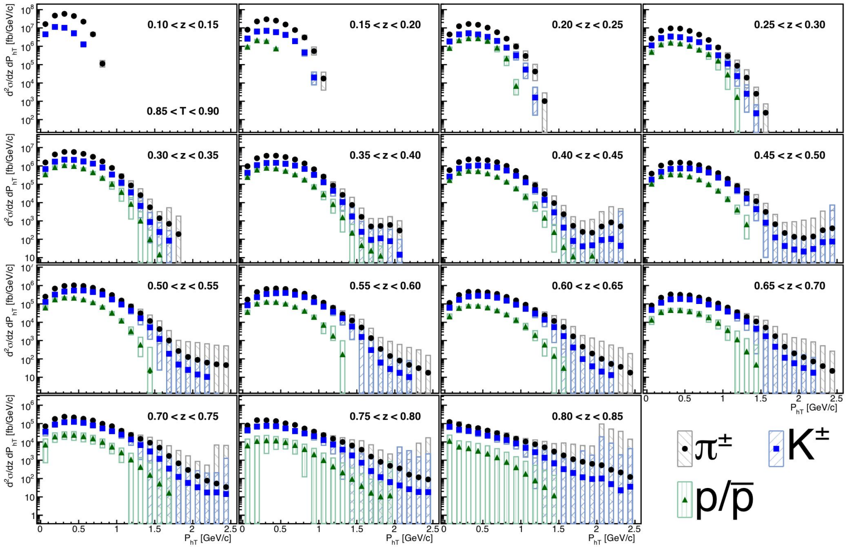

Differential cross sections as a function of transverse momentum

ONGOING RESEARCH

BELLE | $H_1^{\sphericalangle}$ DiFF | JET FUNCTIONS

Back-to-back di-hadron TMD measurements

- A. Vossen, C. van Hulse
- Second hadron provides axis to measure P_{hT}
- Sensitive to the single hadron TMD FF $D_1(z, k_T)$

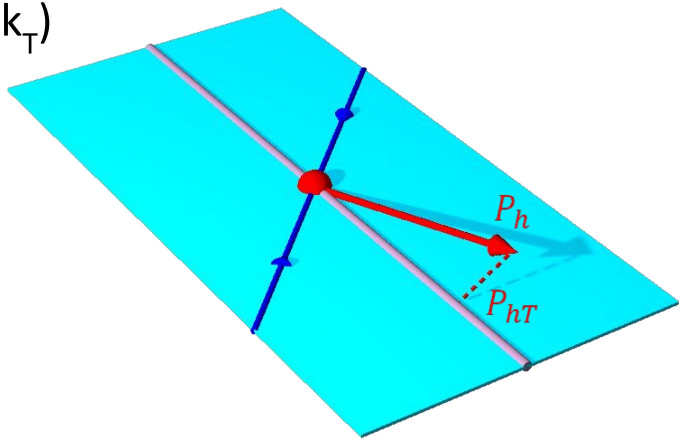

ONGOING RESEARCH

BELLE | $H_1^{\sphericalangle}$ DiFF | JET FUNCTIONS

Production cross-sections of light and charmed mesons (R. Seidl)

- Comprehensive cross section measurements, differential in final hadron momentum
- First measurement of η, K_s^0 at any B-factory, first D_s^{+*} cross-sections at Belle
- Detailed comparison with various MC tunes
- Improved ISR corrections for D-mesons
- Important for SIDIS studies

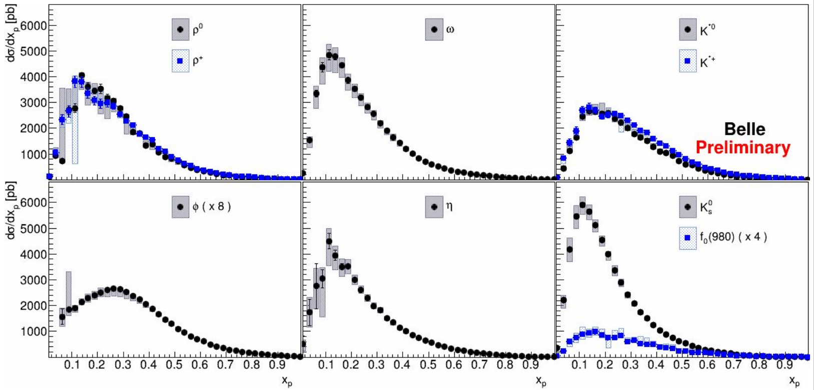

ONGOING RESEARCH

BELLE	$H_1^{\sphericalangle}$ DiFF	JET FUNCTIONS

Production cross-sections of light mesons

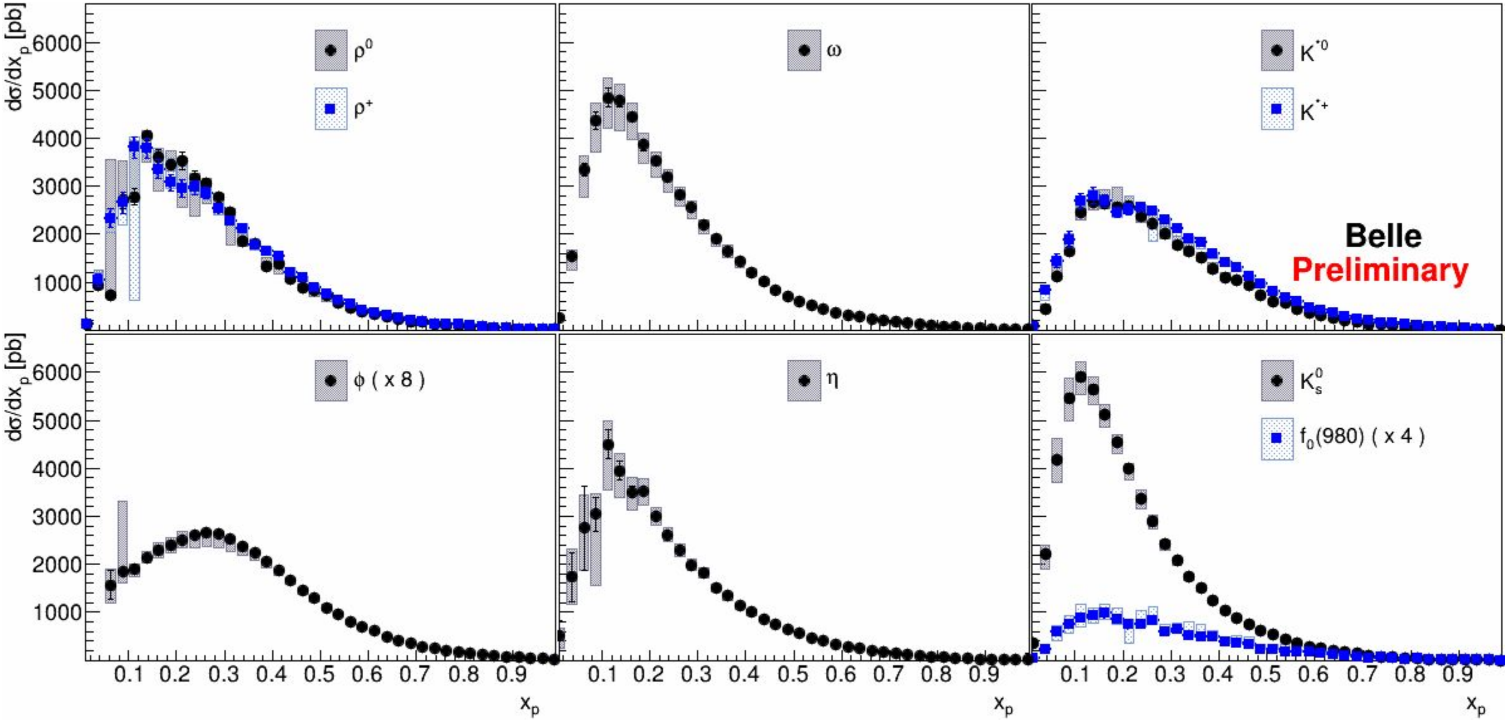

ONGOING RESEARCH

BELLE | $H_1^{\sphericalangle}$ DiFF | JET FUNCTIONS

Production cross-sections of charmed mesons

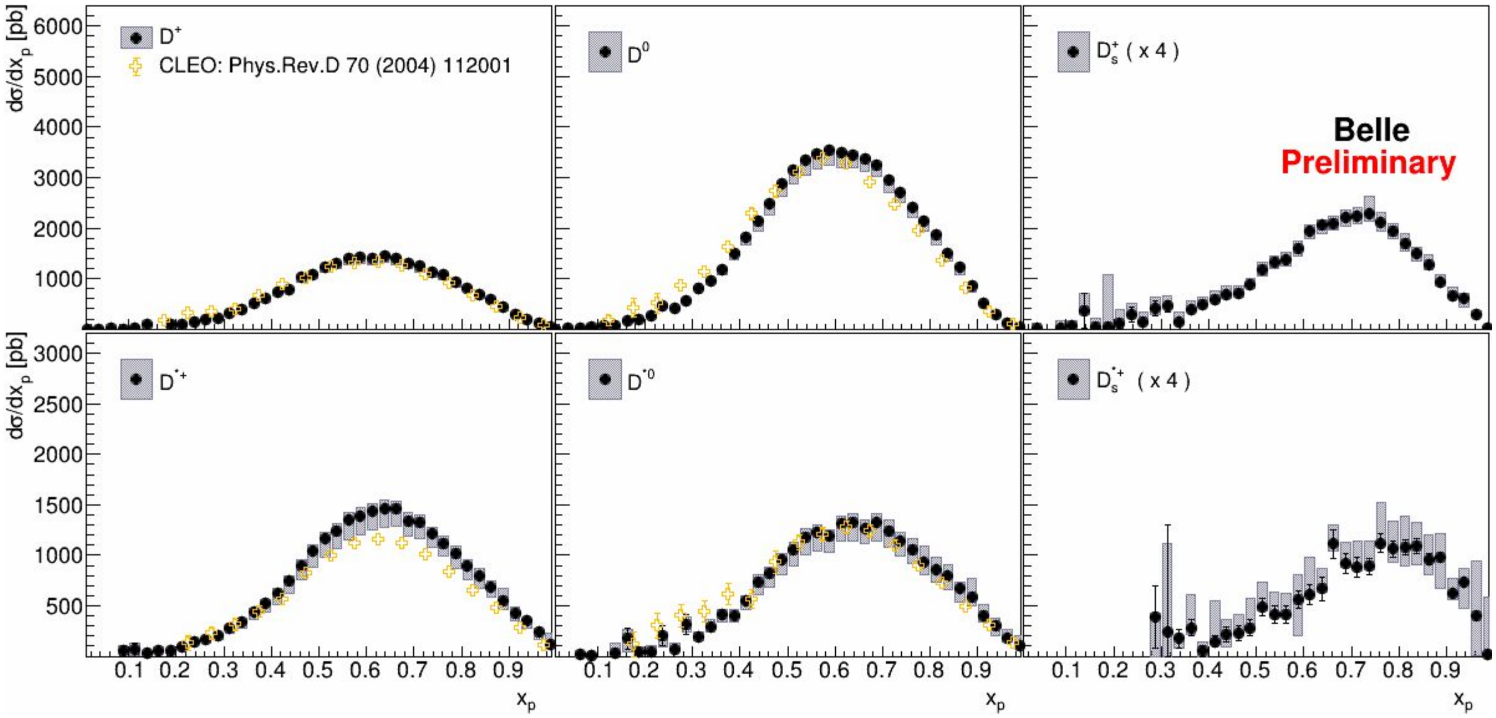

ONGOING RESEARCH

BELLE | $H_1^{\sphericalangle}$ DiFF | JET FUNCTIONS

Production cross-sections of charmed mesons compared to various PYTHIA tunes

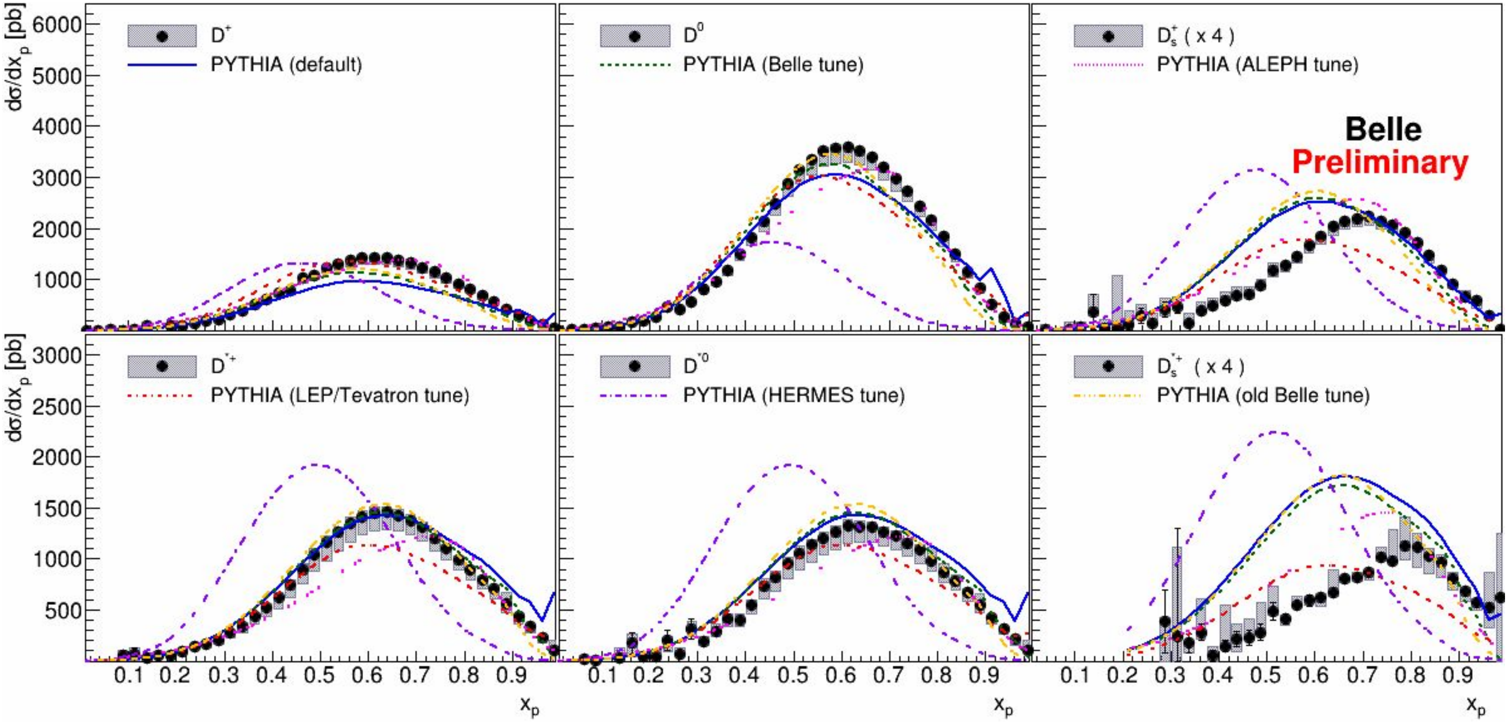

ONGOING RESEARCH

Production cross-sections of light mesons compared to various PYTHIA tunes

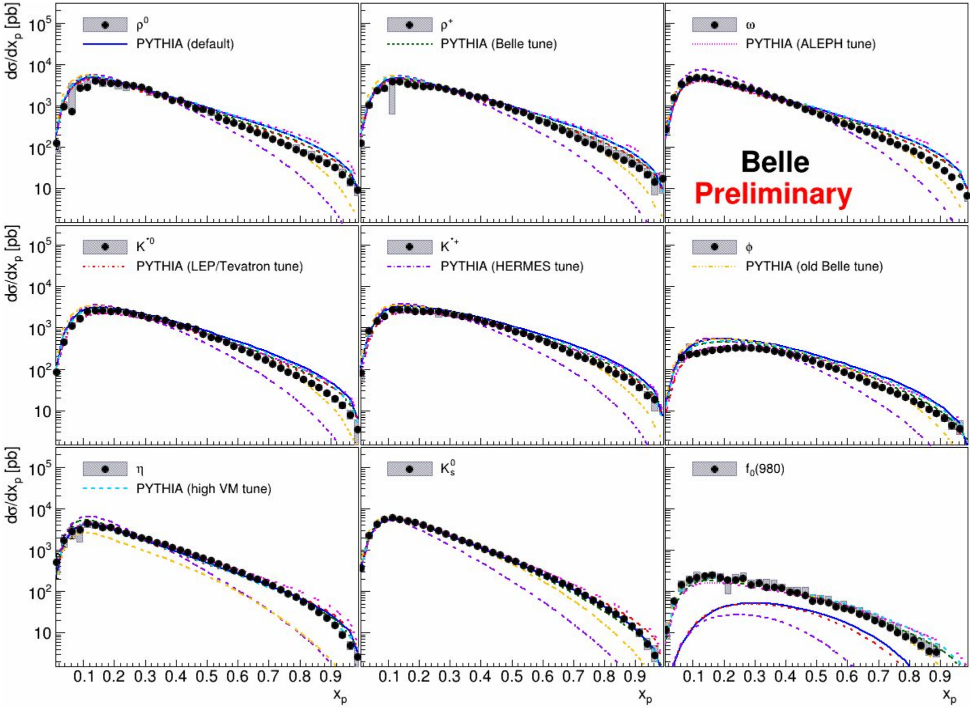

BELLE II STRENGTH: COMPLEX FINAL STATES

DIHADRON FRAGMENTATION FUNCTIONS

Relative momentum between hadrons as additional d.o.f.

More d.o.f's ➞ more information about final state correlations

➞ See e.g. recent extraction of twist-3 e(x) (e-Print: 2203.14975 [hep-ph])

Orientation of two hadrons w.r.t. each other and jet direction as indicator of quark transverse spin

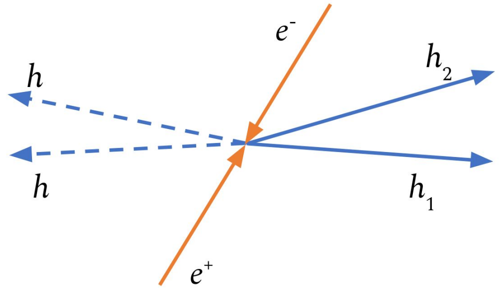

Parton polarization → Hadron Polarization ⇣	Spin averaged	longitudinal	transverse
spin averaged	$D_1^{h/q}(z,M)$		$H_1^{\perp h/q}(z, p_T M, (Ph), \theta)$ 'Di-hadron Collins'
longitudinal			
Transverse		$G_1^{\perp}(z,M,P_h,\theta)=$ T-odd, chiral-even →jet handedness QCD vaccum strucuture	$H_1^{\sphericalangle}(z,M,(P_h),\theta)=$. T-odd, chiral-odd Colinear

BELLE II STRENGTH: COMPLEX FINAL STATES

DIHADRON FRAGMENTATION FUNCTIONS

Relative momentum between hadrons as additional d.o.f.

More d.o.f's ⟶ more information about final state correlations

⟶ See e.g. recent extraction of twist-3 e(x) (e-Print: 2203.14975 [hep-ph])

Orientation of two hadrons w.r.t. each other and jet direction as indicator of quark transverse spin

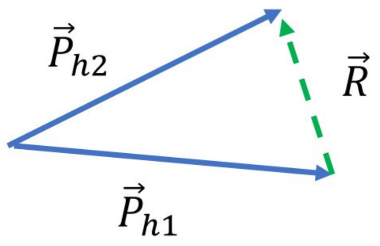

Parton polarization → Hadron Polarization ⇣	Spin averaged	longitudinal	transverse
spin averaged	$D_1^{h/q}(z,M)$		$H_1^{\perp h/q}(z, p_T M, (Ph), \theta)$ 'Di-hadron Collins'
longitudinal			
Transverse		$G_1^{\perp}(z,M,P_h,\theta)$= T-odd, chiral-even →jet handedness QCD vaccum strucuture	$H_1^{\sphericalangle}(z,M,(P_h),\theta)$=. T-odd, chiral-odd Colinear

Work by K. Parham

- The $H_1^{\sphericalangle}$ FF describes the production of a pair of spin-0 hadrons
- Conservation of angular momentum leads to left and right asymmetry
- The spin correlation between a quark-antiquark pair leads to a correlation between the azimuthal angle of the di-hadron pairs it produces
- The amplitude of the resulting asymmetry in the azimuthal angle is directly proportional to $H_1^{\sphericalangle}\overline{H_1^{\sphericalangle}}$

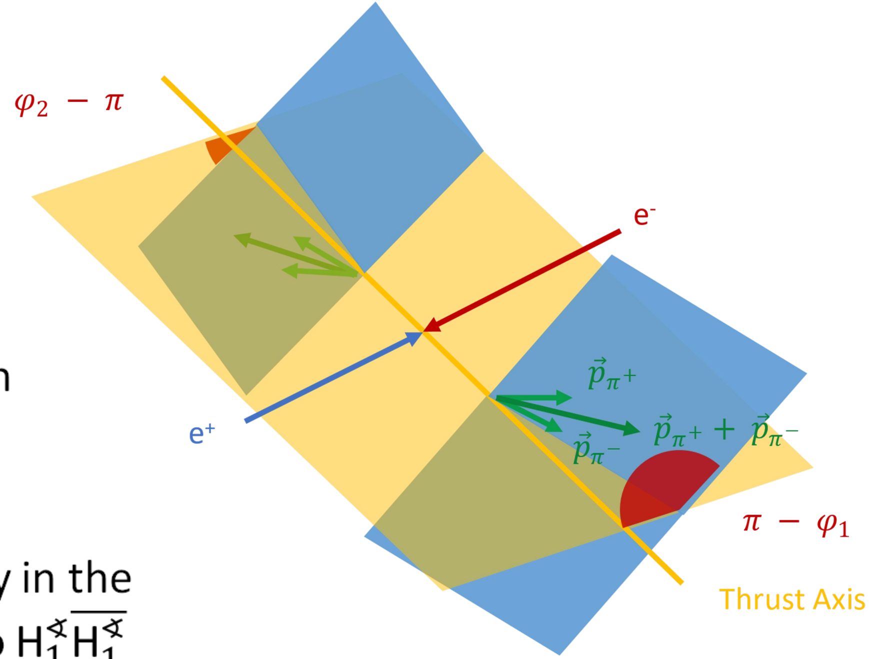

ONGOING RESEARCH

BELLE | $H_1^{\sphericalangle}$ DiFF | JET FUNCTIONS

Azimuthal Asymmetries in $e^+e^- \rightarrow (\pi^+\pi^-)(\pi^+\pi^-)$ Belle Results ($670\ fb^{-1}$):

Asymmetry by Invariant Mass Bins:

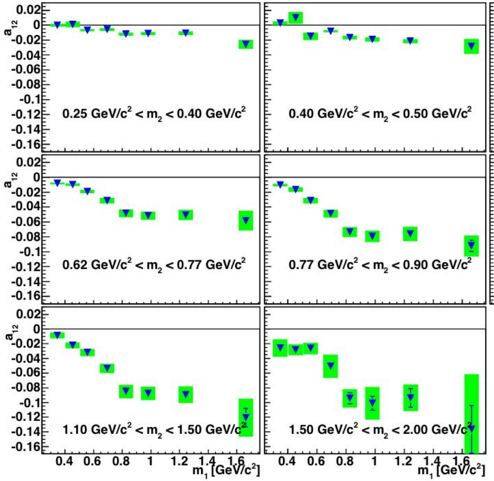

Asymmetry by Pion Fractional Energy Bins:

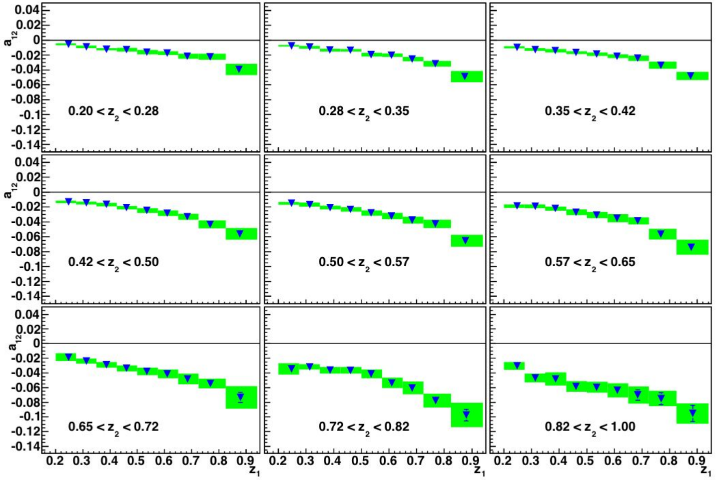

Phys. Rev. Lett. 107, 072004 (2011).

ONGOING RESEARCH

BELLE | $H_1^{\sphericalangle}$ DiFF | JET FUNCTIONS

Work by K. Parham

- Kaon Inclusive
  - The same measurement of $H_1^{\sphericalangle}$ can be made with $K^+ K^-$, $K^+ \pi^-$, or $\pi^+ K^-$ pairs
  - Resulting $H_1^{\sphericalangle}$ measurements could be used to describe the distribution of strange quarks within the nucleon

- Jet Axis
  - Jets are well defined observables and produce better results than the naïve $q\bar{q}$ axis
  - Resulting FFs in e^+e^- are directly connected to FFs in SIDIS

- New measurements are critical to upcoming experiments at JLab and the EIC

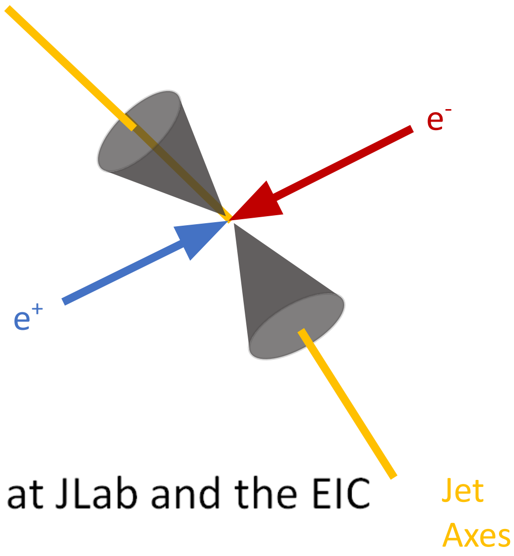

JETS AT B-FACTORIES

DIFFERENCES TO HIGH-ENERGY HADRON COLLISIONS

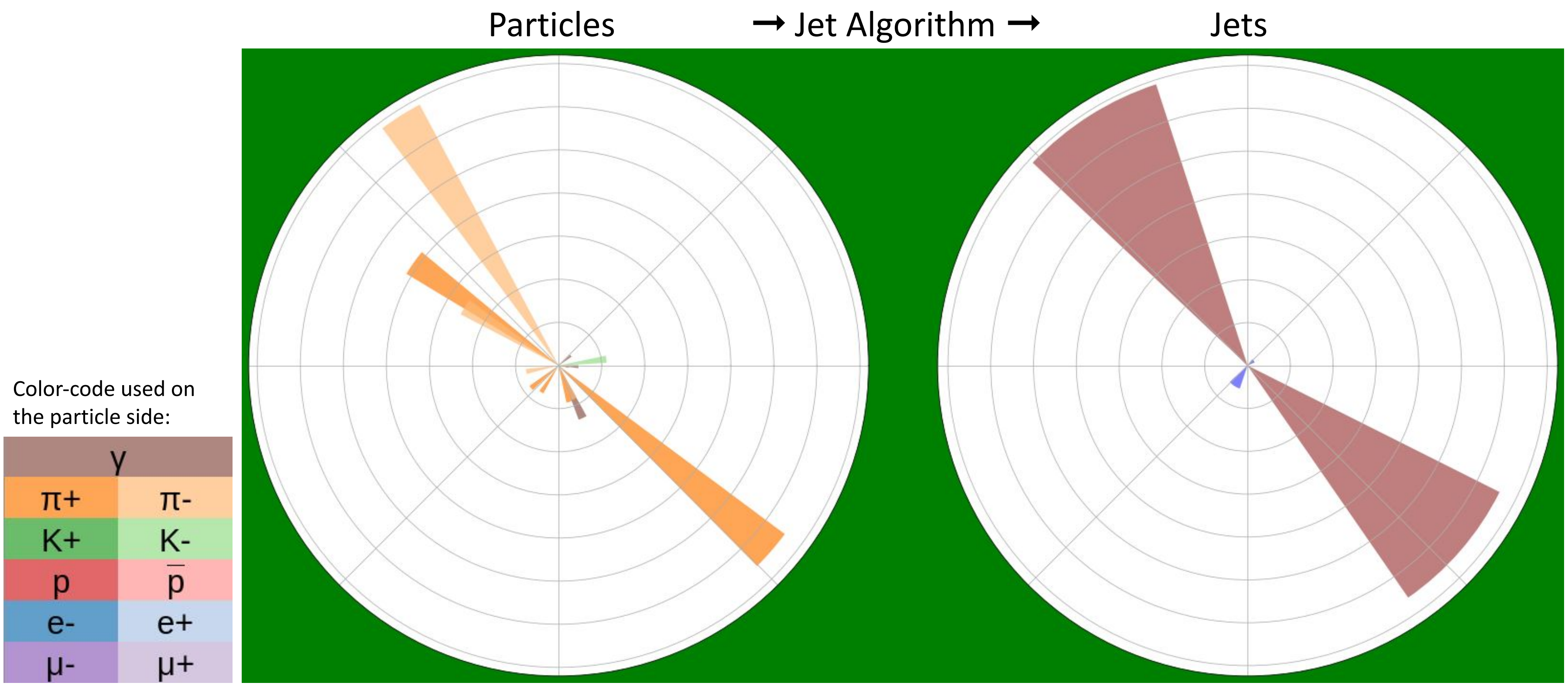

The illustration shows a simulated event projected transverse to the beam direction. The length of the wedges corresponds to the particle’s/jet’s momentum.

ONGOING RESEARCH

- Theoretically, TMD FFs can be replaced by TMD Jet Functions in factorization equations.
  (Gutierrez-Reyes, D., Scimemi, I., Waalewijn, W.J. *et al.)*
- TMD Jet Functions are perturbatively calculable, thus removing a source of uncertainty and allowing greater sensitivity when used to extract PDFs in SIDIS.
- At low momenta, non-perturbative corrections are larger.

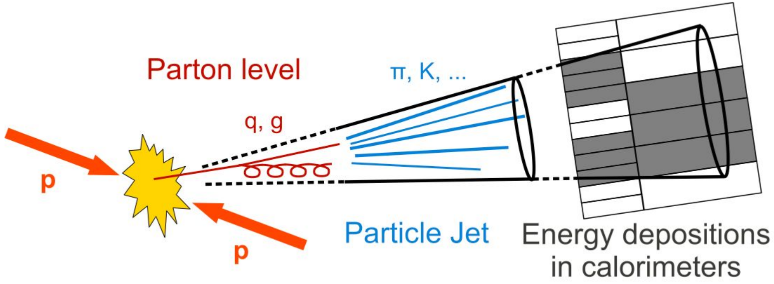

image source: https://cms.cern/news/jets-cms-and-determination-their-energy-scale

ONGOING RESEARCH

BELLE	$H_1^{\sphericalangle}$ DiFF	JET FUNCTIONS

Measuring the jet q_T spectrum:

- Measure the transverse momentum decorrelation, $\boldsymbol{q}$, where $\boldsymbol{p}_i$ are the jet transverse momenta and z_i are their fractional energy:

$$\boldsymbol{q} = \frac{\boldsymbol{p}_1}{z_1} + \frac{\boldsymbol{p}_2}{z_2}$$

- Factorization requires the momentum decorrelation to be small:

$$q_T \equiv |\boldsymbol{q}| \ll \frac{\sqrt{s}}{2}$$

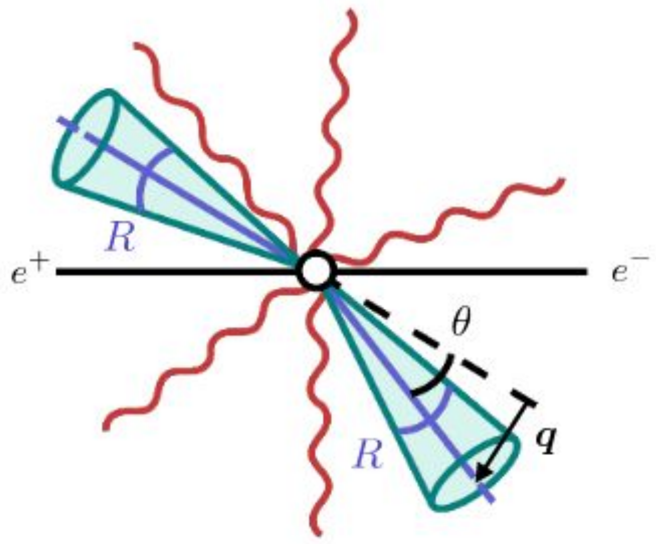

Gutierrez-Reyes, D., Scimemi, I., Waalewijn, W.J. *et al. J. High Energ. Phys.* **2019,** 31 (2019). https://doi.org/10.1007/JHEP10(2019)031

ONGOING RESEARCH

BELLE | $H_1^{\sphericalangle}$ DiFF | JET FUNCTIONS

Theoretical q_T Spectrum at Belle II and LEP

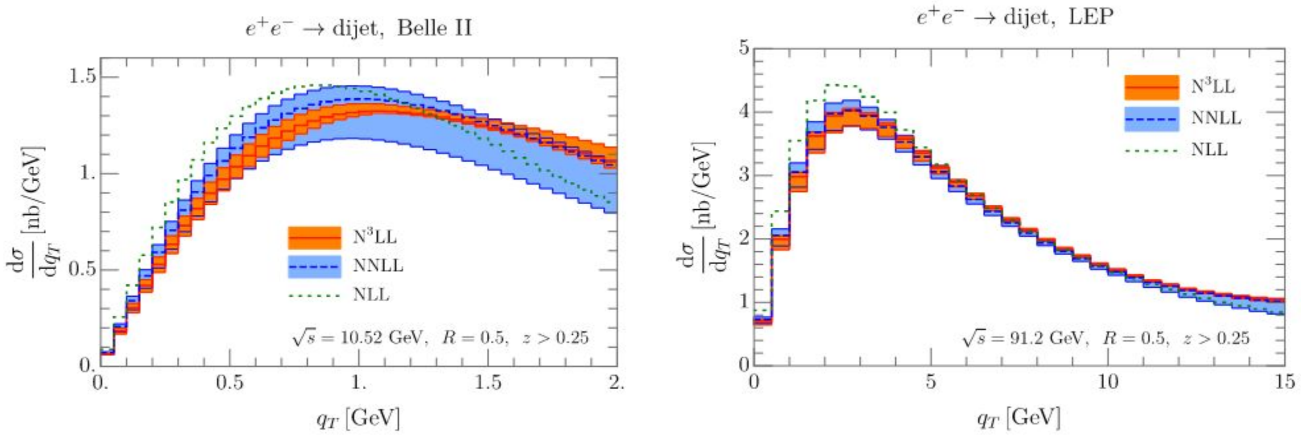

Figure 5. Perturbative convergence of the cross section differential in transverse momentum decorrelation, for Belle II (left) and LEP (right), for jet radius $R = 0.5$ and jet energy fraction $z > 0.25$. The N^{3}LL result is obtained with the prescription in eq. (6.1). The bands encode the perturbative uncertainty, as described in the text.

Gutierrez-Reyes, D., Scimemi, I., Waalewijn, W.J. *et al. J. High Energ. Phys.* **2019,** 31 (2019). https://doi.org/10.1007/JHEP10(2019)031

ONGOING RESEARCH

BELLE | $H_1^{\sphericalangle}$ DiFF | JET FUNCTIONS

Theoretical q_T Spectrum at Belle II and LEP

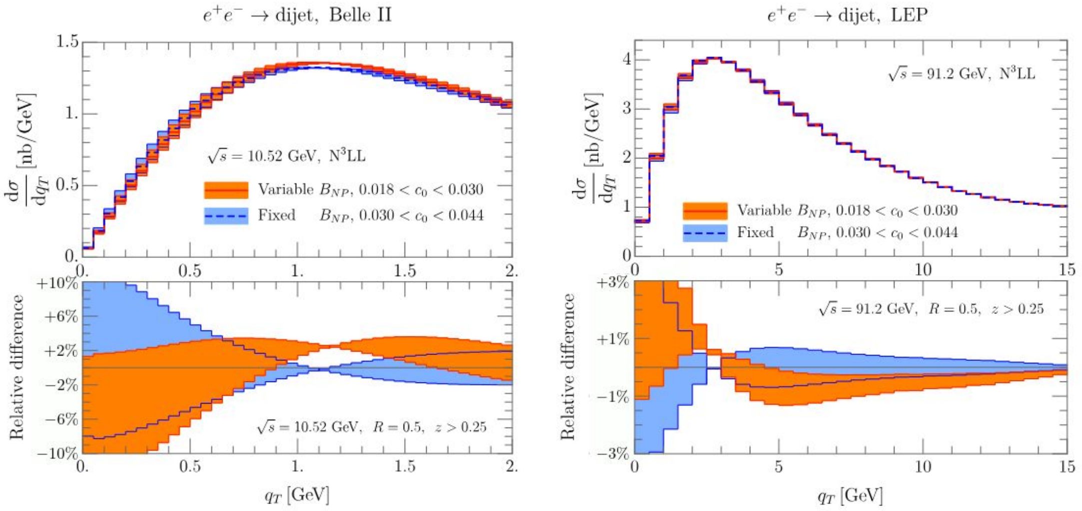

Figure 7. Estimate of the sensitivity of the TMD to nonperturbative effects in the rapidity resummation at Belle II (left) and LEP (right). We vary the parameter c_0 in the range of its statistical uncertainty, testing both the fixed and variable $B_{\rm NP}$ schemes of ref. [56]. Results are obtained with the prescription in eq. (6.1).

Gutierrez-Reyes, D., Scimemi, I., Waalewijn, W.J. *et al. J. High Energ. Phys.* **2019,** 31 (2019). https://doi.org/10.1007/JHEP10(2019)031

ONGOING RESEARCH

- The time reversal-odd (T-odd) components of a jet were thought to vanish, but were recently found to survive due to non-perturbative effects.

- T-odd jet structure plays an important role in accessing nucleon spin structures.

- In particular, the T-odd constituent can couple to the proton transversity at the EIC.

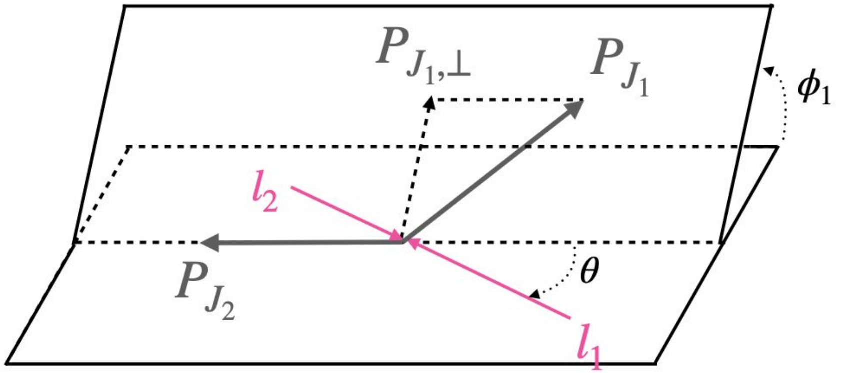

$$R^{J_1 J_2} = 1 + \cos(2\phi_1)\frac{\sin^2\theta}{1+\cos^2\theta}\frac{F_T(q_T)}{F_U(q_T)}$$

Liu, X., Xing, H. *The Time-reversal Odd Side of a Jet* arXiv:2104.03328

Near-future opportunities with Belle II data

Some highlights

- 1st generation B-factory data insufficient for EIC program
    - e.g. higher dim. binnings
- Improved vertexing to allow separation of charm contributions
- Heavy flavor fragmentation studies
- Di-hadron production
    - ➞ Including partial wave analysis
- Interrelations with MC modelling
- For more information, see recent Belle II QCD whitepaper:
    - (arXiv:2204.02280 [hep-ex])

SUMMARY

- Belle and Belle II data plays important role in the direct study of QCD
    - Demonstrated e.g. by recent Belle publications
- Key ingredient to extract nucleon structure in SIDIS (e.g. at the EIC)
    - Planned datasets to improve on 1st gen by order of magnitude
- Advances in theory and phenomenology motivate analyses with new tools
- A rich QCD program has been formulated for Belle II, with several analyses under way

Thanks for help in preparing this presentation to K. Parham, A. Vossen, R. Seidl,
and the Belle II collaboration!